Elevate Series

ORIGINAL RESEARCH

Prognostic Role of SETDB2 in Clear Cell Renal Cell Carcinoma: Linking Immune Infiltration, Cuproptosis, and Tumor Suppression

Si Hao Lu[1],*, Kui Lui[1],*, Yue Qian[2], Wei ye Zhou[3], Ying Ying Mu[4], Wei Zhang [2,3]

[1]Department of Nephrology, Air Force Hospital of Western Theater Command, Chengdu, 610000, People's Republic of China; [2]Department of Pathogen Biology, Guizhou Nursing Vocational College, Guiyang, Guizhou, 550000, People's Republic of China; [3]Cell Biology Department, Wuxi School of Medicine, Jiangnan University, Wuxi, Jiangsu, 214122, People's Republic of China; [4]Department of Pathology, Zunyi Hospital of Traditional Chinese Medicine, Zunyi, Guizhou, 563000, People's Republic of China

*These authors contributed equally to this work

Correspondence: Wei Zhang, Department of Pathogen Biology, Guizhou Nursing Vocational College, Guiyang, Guizhou, 550000, People's Republic of China, Email lawrence2013@163.com

Background: Clear cell renal cell carcinoma (ccRCC) is a relatively frequently diagnosed form of urological cancer that is highly malignant and associated with high rates of patient mortality. At present, there are few effective options for treating advanced cases of ccRCC, emphasizing the need to establish novel biomarkers and targets suitable for therapeutic intervention. SET domain bifurcated histone lysine methyltransferase 2 (SETDB2) belongs to the Su(var)3–9 subfamily of methyltransferases and has been linked to various forms of cancer, but the role it plays in ccRCC remains to be fully established.

Methods: Data on SETDB2 expression were downloaded from The Cancer Genome Atlas (TCGA) and Gene Expression Omnibus (GEO) databases. Functional enrichment analyses were then used to probe the putative role that SETDB2 plays in the onset of ccRCC. The Gene Set Cancer Analysis (GSCA) platform and molecular docking analysis were utilized to investigate the relationship between gene expression and drug sensitivity. In the end, the core target and the active molecule were both given the green light for a molecular docking investigation. Functional assays and Western blotting performed with ccRCC cell lines were employed for the validation of the findings from these predictive analyses.

Results: SETDB2 downregulation was observed in ccRCC, and lower levels were found to linked with poor patient outcomes. Lower SETDB2 levels were associated with worse overall, progression-free, and disease-specific survival. In Functional enrichment analyses, SETDB2 was predicted to regulate key ccRCC development-associated pathways. SETDB2 levels were also significantly associated with cuproptosis induction in KIRC tissues, while in immune cell infiltration analyses, SETDB2 expression was linked with immune responses within the tumor microenvironment. Functional experiments conducted with ccRCC cell lines unveiled molecular mechanisms through which SETDB2 appears to be capable of inhibiting the development of ccRCC.

Conclusion: Together, these analyses highlight the utility of SETDB2 as a prognostic biomarker in ccRCC. The interactions and associated pathways detected through these analyses provide unique insight into the potential functions of SETDB2 in this cancer type, providing an evidence base for future studies.

Keywords: SETDB2, biomarkers, kidney renal clear cell carcinoma, prognosis, tumor-immune infiltration, cuproptosis

Introduction

Renal cell carcinoma (RCC) is relatively common urological tumor, representing ~3% of global cancer cases, with an estimated 400,000 diagnoses per year and a mortality rate as high as 40%.[1] Over the past two decades, a steady 2% annual increase in RCC incidence has been observed.[2] Clear cell RCC (ccRCC) is the most prevalent and deadliest RCC subtype, making up 70–75% of all cases.[3] In its early stages, ccRCC treatment consists primarily of surgery, and patient survival rates are approximately 60–70%.[4,5] Advanced ccRCC, however, is characterized by 5-year survival rates in the 10% range in some instances despite efforts to develop reliable treatments, underscoring the poor prognosis associated with this malignancy.[6–8] The molecular drivers of ccRCC remain poorly understood, and the absence of accurate molecular targets or clinical biomarkers

675

persistently hampers efforts to diagnose and treat this disease. The establishment of new biomarkers and therapeutic targets is thus vital to the improvement of ccRCC patient diagnosis in the early stages of disease and to achieve a better overall prognosis, as these findings may help design more effective interventional strategies that yield more favorable patient outcomes.

The histone methyltransferase SETDB2 catalyzes the trimethylation of histone H3 lysine 9 (H3K9me3). It consists of a segmented SET region, a preSET region, and a methylated CpG binding region.[9,10] High levels of SETDB2 expression have been reported in gastric cancer, and it can promote tumor cell invasivity and migratory activity through its ability to silence CADM1 and WWOX, which are tumor suppressor genes.[11] SETBD2 expression dynamics in ccRCC, however, remain uncertain, as to the mechanisms through which it impacts the invasion and metastasis of ccRCC cells.

To address these areas of uncertainty, in this study, SETDB2 expression in kidney renal clear cell carcinoma (KIRC) was analyzed, and the association between SETDB2 levels and various clinical parameters was evaluated. A protein-protein interaction (PPI) network incorporating SETDB2 and associated differentially expressed genes (DEGs) was also constructed. The further characterize the function of this gene, the relationships between SETDB2 levels, immune cell invasion, immune status-related gene sets, and cuproptosis were assessed through the use of multiple databases. The role that SETDB2 plays in KIRC development was predicted through the integration of signaling pathway enrichment and immune infiltration analyses. The overall objective of these analyses was to clarify the specific mechanistic function of SETDB2 in ccRCC development and to clarify its utility as a target for therapeutic intervention.

Methods
Data Collection
The UCSC TCGA Pan-Cancer database (https://xenabro wser.net/) was accessed to obtain the pan-cancer dataset used for analyses in this study, which included gene expression, prognosis-related, and immune-related analyses. The Cancer Genome Atlas (TCGA) was accessed to obtain the TCGA-KIRC database used to conduct gene expression and clinicopathological analyses. Analyses of SETDB2 expression levels in KIRC were performed using the Gene Expression Omnibus GSE53757 and GSE40435 datasets. The Human Protein Atlas (HPA) is a database with immuno-histochemical (IHC) data corresponding to 17 major cancer types and 44 normal tissue types.[12]

Prognosis Analysis
Univariate Cox regression analyses were used to assess overall survival (OS), disease-specific survival (DSS), and progression-free interval (PFI) curves for STAD, COAD, HNSC, LUSC, LIHC, KIRC, KICH, CHOL, and THCA, visualizing the results with forest plots incorporating the corresponding P-values, hazard ratios (HRs), and 95% confidence intervals (CIs). The R 'forstplot' package was utilized to perform these analyses. SETDB2 expression levels in KIRC samples were used to generate Kaplan-Meier plots using the R 'survival' and 'survminer' packages.

Analyses of Genetic Alteration
The frequencies of SETDB2 mutation, copy number changes, and mutation types across KIRC Atlas studies were assessed with cBioPortal (https://www.cbiopo rtal.org/).[13] Specific mutation types were additionally evaluated with the Catalogue of Somatic Mutations in Cancer (COSMIC).

Functional Enrichment Analyses
Data pertaining to the top 200 genes showing closest associations with SETDB2 were collected, and correlations between the expression of SETDB2 and the top four most closely correlated genes were identified using GEPIA2 (https://gepia2. cancer-pku.cn/),[14,15] which enables analyses of transcriptomic data from the TCGA and GTEx projects. SETDB2 PPI network establishment was performed with STRING (https://string-db.org/).[16] To develop this network, the "Search" module was searched for the protein (SETDB2) and organism (Homo sapiens), with all settings other than the following at default values: minimum required interaction score ("low confidence (0.150)"), active interaction source ("Textmining and experiment"), and ≤ 50 interactors in the first shell. The two sets of information were integrated to conduct Gene Ontology (GO) and KEGG functional enrichment analyses.

Immune Cell Infiltration Analyses

Correlations between SETDB2 and six different tumor-infiltrating immune cell types (CD4+ T cells, CD8+ T cells, B cells, dendritic cells [DCs], neutrophils, and macrophages) were assessed with TIMER (https://cistrome.shinyapps.io/timer/). Associations between immune cell responses and SETDB2 levels in KIRC were additionally analyzed using CIBERSORT (Newman et al, 2015), setting $P < 0.05$ as significant. The ESTIMATE algorithm[17] was applied to assess links between SETDB2 levels and the immune, stromal, and ESTIMATE scores for each KIRC sample.

Immune Checkpoint and TMB Correlation Analyses

Correlations between SETDB2 and immune checkpoints in KIRC were assessed with the R 'limma' and 'corrplot' packages based on TCGA data, regarding $P < 0.001$ as the cut-off for significance. The 'limma' package was also used to examine correlations between SETDB2 levels and tumor mutational burden (TMB).

Drug Sensitivity Analysis

The effect of SETDB2 on drug susceptibility was evaluated using the GSCA (Gene Set Cancer Analysis) (http://bioinfo.life.hust.edu.cn/GSC-A/#/)[18] and the Genomics of Drug Sensitivity in Cancer (GDSC) databases.

Molecular Docking Analysis of Lapatinib with SETDB2

Molecular docking simulations were conducted to predict the interaction patterns between the active sites of proteins and ligands using Schrödinger Suite Maestro (Version 11.5). Protein structures for these hub genes and drugs were obtained from the RCSB Protein Data Bank (RCSB PDB) (https://www.rcsb.org/), SWISS-MODEL server (https://swissmodel.expasy.org/), and PubChem (https://pubchem.ncbi.nlm.nih.gov/). The collected data were processed and visually presented according to a previously reported study.[19] Subsequently, PyMOL software (version 2.3) was employed to derive the affinity parameters and 3D spatial structures based on the calculated binding energies.

Cell Culture

786–0 and Caski-1 cells from Procell Life Science & Technology Co., Ltd (CL-0010; CL-0052, Wuhan, China) were grown in DMEM with 10% FBS in a 5% CO_2 37°C incubator.

Transfection

The SETDB2-overexpression plasmid (OE-SETDB2) and the negative control NC recombinant plasmid (NC-SETDB2) were obtained from Gima Gene (Shanghai, China). KIRC cells were transfected with these plasmids with Lipofectamine 6000 (Beyotime Biotechnology, Shanghai, China) as directed, after which cells were cultured for 48 h. Four replicates were established for all experiments.

Western Immunoblotting

RIPA buffer (P0013B, Beyotime Biotechnology) with PMSF (ST506) and phosphatase inhibitors (P1081) was used to lyse KIRC cell lines, followed by their electrophoretic separation on SDS-PAGE gels and transfer to PVDF membranes (0.45 μm; Merck Millipore, MA, USA). Following a 1 h block step using 5% BSA, blots were treated with rabbit anti-SETDB2 (14,428-1-AP, Proteintech Group, Inc, Wuhan, China; 1:1000) and rabbit anti-GAPDH (K110496P, Solarbio, Beijing, China; 1:2000), and they were then incubated in the presence of secondary antibodies. A Tanon-2500B gel imaging analysis system (Tanon, Shanghai, China) was used for protein quantification, using ImageJ (V1.6, NIH, MD, USA) for densitometric analyses of signal intensity.

CCK-8 Assay

A CCK-8 assay (Cat No. CA1210; Solarbo, Beijing, China) was used as directed to assess growth inhibition. Briefly, after adding cells to 96-well plates ($5x10^3$/well) in six replicate wells, cells were incubated for 48 h post-transfection, followed by the addition of CCK-8 reagent (10 μL/well). Absorbance at 450 nm was then quantified following a 1 h incubation at 37°C.

Wound Healing Assay

786–0 and Caski-1 cells were added to 6-well plates at 48 h post-transfection, and when they were 90% confluent, the monolayer was scratched with a 10 μL, culturing the remaining cells in serum-free DMEM and imaging the wounded area after 0, 24, and 48 h.

Transwell Assays

Serum-free DMEM was used to suspend cells, followed by the addition of 3×10^4 cells in 100 μL to the upper chamber of a Transwell insert, whereas 600 μL of media with 10% FBS was added in the lower chamber. After 48 h at 37°C, crystal violet solution (C0121, Beyotime Biotechnology) was used to stain cells, followed by their observation under a light microscope.

Statistical Analyses

R v 4.0.3 was used for analyses of bioinformatics data. Results were reported as means ± SEM, and were compared with t-tests or one-way ANOVAs, defining $P < 0.05$ as the cut-off for significance. The associations between SETDB2 expression and patient characteristics were assessed through Wilcoxon rank-sum, Fisher's exact, chi-square, and logistic regression tests.

Results

SETDB2 is Downregulated in Multiple Types of Cancer

Using the TIMER 2.0 tool, SETDB2 expression was initially compared in several forms of cancer. Of these analyzed cancer types, significant SETDB2 downregulation was noted in BLCA, BRCA, KIRC, KIRP, LUJAD, THCA, LUSC, PRAD, UCEC, and SKCM, relative to their corresponding normal control tissue types. However, SETDB2 upregulation was instead noted in STAD, LIHC, and CHOL (Figure 1A).

Paired data analyses yielded similar results when comparing SETDB2 expression levels specifically between tumors and paired normal tissue samples (Figure 1B). SETDB2 downregulation was observed in BRCA KIRC, LUAD, LUSC, THCA, and UCEC relative to their normal tissue controls, whereas it was upregulated in CHOL, COAD, and LIHC. The GTEx and TCGA databases were also leveraged to assess SETDB2 levels. Reduced SETDB2 levels were noted in all analyzed tumor tissue types relative to corresponding normal tissue controls, including in ACC, BLCA, BRCA, CESC, KIRC, LUAD, LUSC, OV, THCA, PRAD, UCS, UCEC, PCRD, and TGCT (Figure 1C).

SETDB2 Expression is Related to Tumor Patient Prognostic Outcomes

In differential expression analyses, SETD2 levels were significantly associated with several types of cancer including BRCA, KIRC, LUSC, OV, UCEC, and THCA. This finding prompted a further investigation of the prognostic value of SETDB2 levels in these tumor types in the form of survival analyses (Figure 2). Marked differences in patient OS as a function of SETDB2 expression were observed in KIRC ($p < 0.001$), KIRP ($p < 0.05$), LGG ($p < 0.01$), LUAD ($p < 0.01$), and PAAD ($p < 0.05$) (Figure 2A), indicating SETDB2 influence on survival in these malignancies. Similarly, DSS analyses supported a key role for SETDB2 levels in KIRC, KIRP, LGG, PAAD, and READ patient outcomes (Figure 2B), with lower SETDB2 levels being positively correlated with poor outcomes in KIRC (p=4.13e-05; HR 0.425), KIRP (p=0.0022; HR 0.245), and PAAD (p=0.0172; HR 0.567), whereas it was negatively associated with these outcomes in LGG (p=0.0018; HR 1.79). SETDB2 levels were also significantly associated with the progression-free interval (PFI) for patients with KIRC (p=3.2e-06; HR 0.456), LGG (p=0.0150; HR 1.407), PAAD (p=0.0320; HR 0.656), and THCA (p=0.0306; HR 0.540) (Figure 2C). Together, these results support the significant impact that SETDB2 can have on KIRC patient prognostic outcomes when analyzing several different survival metrics, emphasizing the need for further analyses exploring the role that SETDB2 plays in KIRC in light of its clear clinical relevance.

SETDB2 is Downregulated in KIRC

To gain more direct insight into the clinical and biological significance of SETDB2 in KIRC, the TCGA-KIRC dataset and GTEx database were next analyzed. This approach revealed significantly decreased SETDB2 expression in KIRC
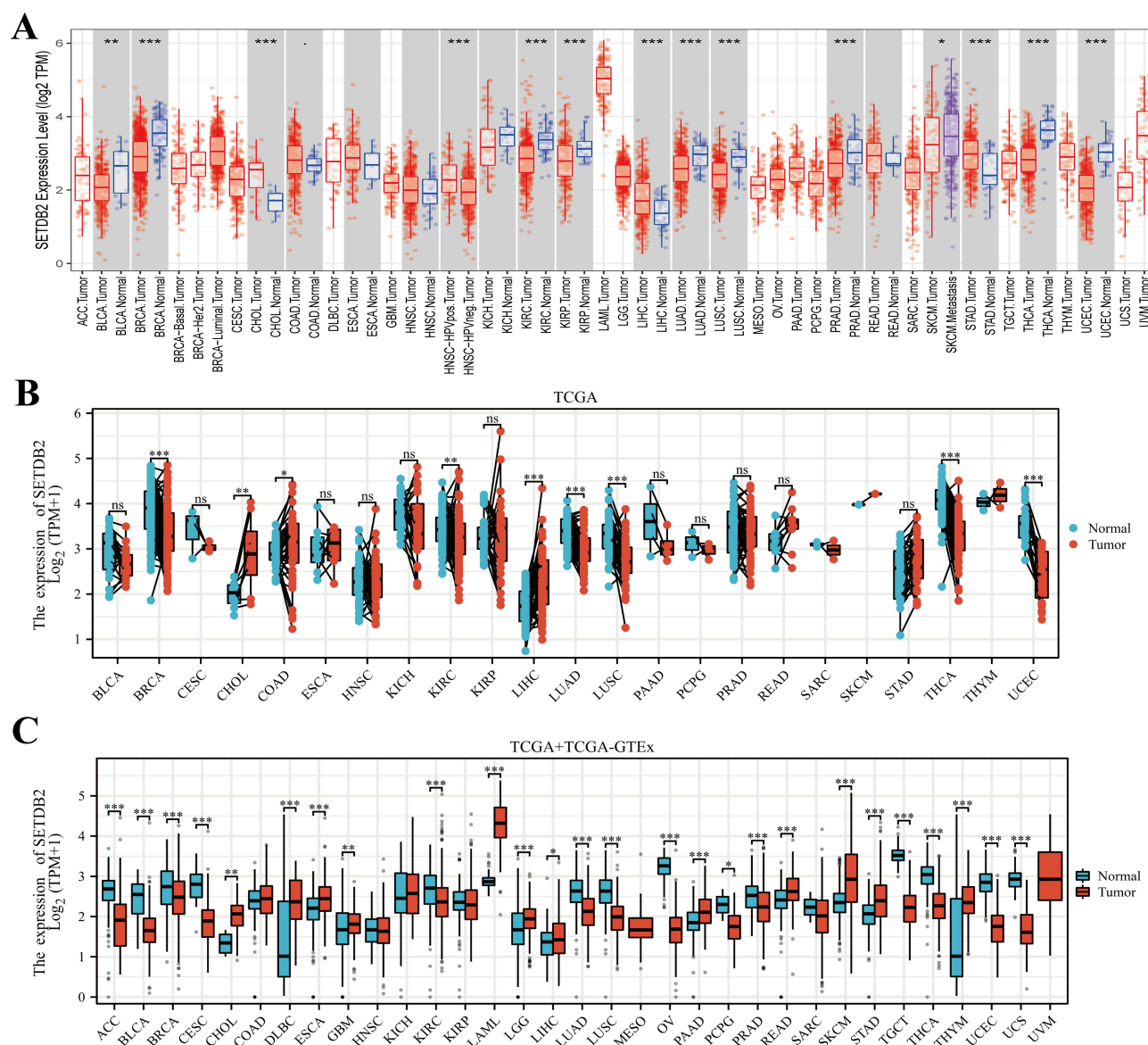
Figure 1 Pan-cancer analysis of SETDB2 expression. (**A**) SETDB2 levels in tumors and paracancerous tissues from different tumor types included in the TCGA database, based on TIMER2.0 analyses. (**B**) Pan-cancer and paired normal tissue SETDB2 levels in TCGA data. (**C**) Comparisons in SETDB2 levels between the GTEx and TCGA databases, as analyzed with Wilcoxon rank-sum tests. *, $p < 0.01$; **, $p < 0.01$; ***, $p < 0.001$; ns, no significance.
Abbreviation: TPM, transcripts per million.

samples relative to normal controls ($p < 0.001$; Figure 3A and B), and pairwise comparisons of tumor and paracancerous tissues similarly supported its downregulation in tumors ($p < 0.05$; Figure 3C). Comparable SETDB2 downregulation in KIRC tissues was also noted in the GSE53757 and GSE40435 datasets ($p < 0.05$; Figure 3D and E). The Human Protein Atlas also noted significant SETDB2 protein downregulation in KIRC tissues relative to normal control tissues (Figure 3F). These results strongly demonstrate that SETDB2 is downregulated in the tumors of KIRC patients.

Low SETDB2 Levels are Linked to Poor KIRC Patient Clinicopathological Features

The TCGA-KIRC dataset was further employed to investigate the link between SETDB2 mRNA expression and patient clinicopathological characteristics. These analyses supported a significant association between SETDB2 mRNA levels and pathological T stage (Figure 4A), M stage (Figure 4B), overall pathologic stage (Figure 4C), histologic grade (Figure 4D), and age (Figure 4E). In contrast, they were not significantly related to pathologic N stage (Figure 4F). SETDB2 thus offers potential utility as a biomarker of aggressive KIRC tumor growth.
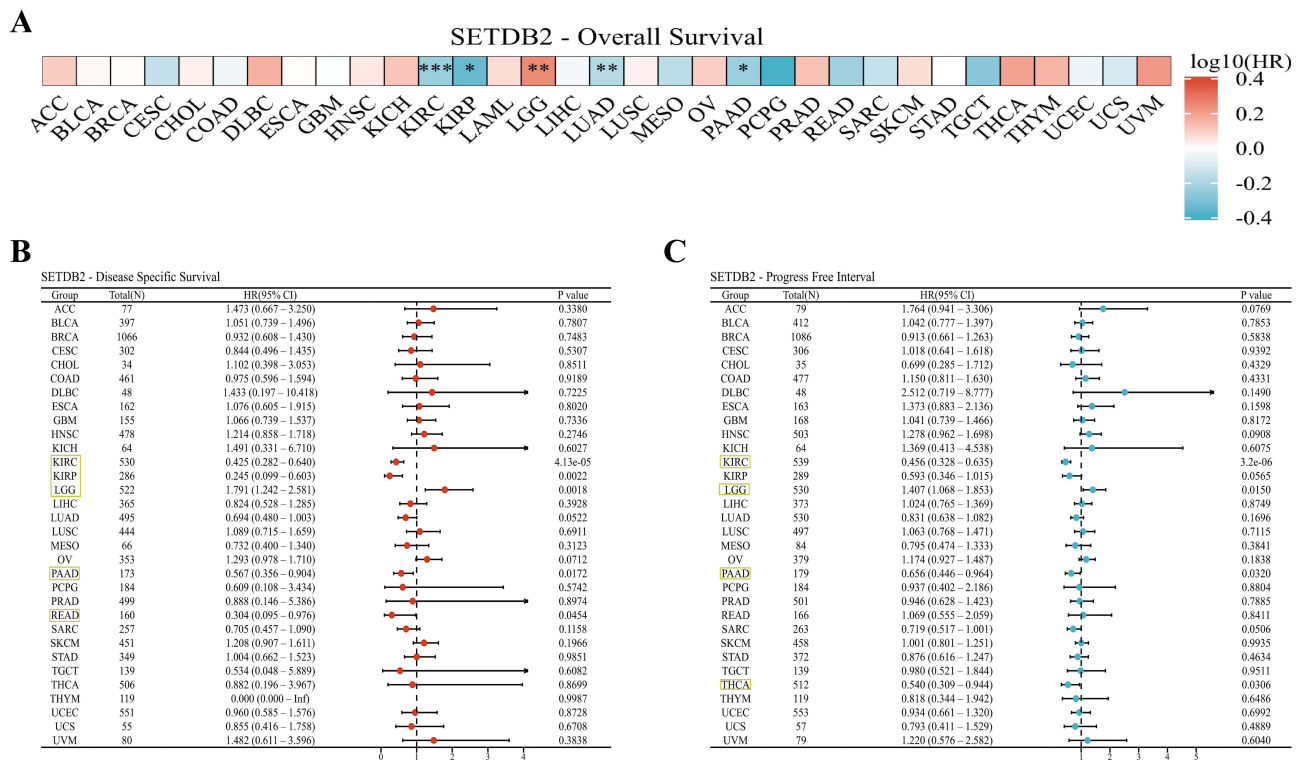
A

SETDB2 - Overall Survival

ACC BLCA BRCA CESC CHOL COAD DLBC ESCA GBM HNSC KICH KIRC(***) KIRP(*) LAML LGG(**) LIHC LUAD LUSC(**) MESO OV PAAD PCPG(*) PRAD READ SARC SKCM STAD TGCT THCA THYM UCEC UCS UVM

log10(HR)
0.4
0.2
0.0
-0.2
-0.4

B

SETDB2 - Disease Specific Survival

Group	Total(N)	HR(95% CI)		P value
ACC	77	1.473 (0.667 – 3.250)		0.3380
BLCA	397	1.051 (0.739 – 1.496)		0.7807
BRCA	1066	0.932 (0.608 – 1.430)		0.7483
CESC	302	0.844 (0.496 – 1.435)		0.5307
CHOL	34	1.102 (0.398 – 3.053)		0.8511
COAD	461	0.975 (0.596 – 1.594)		0.9189
DLBC	48	1.433 (0.197 – 10.418)		0.7225
ESCA	162	1.076 (0.605 – 1.915)		0.8020
GBM	155	1.066 (0.739 – 1.537)		0.7336
HNSC	478	1.214 (0.858 – 1.718)		0.2746
KICH	64	1.491 (0.331 – 6.710)		0.6027
KIRC	530	0.425 (0.282 – 0.640)		4.13e-05
KIRP	286	0.245 (0.099 – 0.603)		0.0022
LGG	522	1.791 (1.242 – 2.581)		0.0018
LIHC	365	0.824 (0.528 – 1.285)		0.3928
LUAD	495	0.694 (0.480 – 1.003)		0.0522
LUSC	444	1.089 (0.715 – 1.659)		0.6911
MESO	66	0.732 (0.400 – 1.340)		0.3123
OV	353	1.293 (0.978 – 1.710)		0.0712
PAAD	173	0.567 (0.356 – 0.904)		0.0172
PCPG	184	0.609 (0.108 – 3.434)		0.5742
PRAD	499	0.888 (0.146 – 5.386)		0.8974
READ	160	0.304 (0.095 – 0.976)		0.0454
SARC	257	0.705 (0.457 – 1.090)		0.1158
SKCM	451	1.208 (0.907 – 1.611)		0.1966
STAD	349	1.004 (0.662 – 1.523)		0.9851
TGCT	139	0.534 (0.048 – 5.889)		0.6082
THCA	506	0.882 (0.196 – 3.967)		0.8699
THYM	119	0.000 (0.000 – Inf)		0.9987
UCEC	551	0.960 (0.585 – 1.576)		0.8728
UCS	55	0.855 (0.416 – 1.758)		0.6708
UVM	80	1.482 (0.611 – 3.596)		0.3838

C

SETDB2 - Progress Free Interval

Group	Total(N)	HR(95% CI)		P value
ACC	79	1.764 (0.941 – 3.306)		0.0769
BLCA	412	1.042 (0.777 – 1.397)		0.7853
BRCA	1086	0.913 (0.661 – 1.263)		0.5838
CESC	306	1.018 (0.641 – 1.618)		0.9392
CHOL	35	0.699 (0.285 – 1.712)		0.4329
COAD	477	1.150 (0.811 – 1.630)		0.4331
DLBC	48	2.512 (0.719 – 8.777)		0.1490
ESCA	163	1.373 (0.883 – 2.136)		0.1598
GBM	168	1.041 (0.739 – 1.466)		0.8172
HNSC	503	1.278 (0.962 – 1.698)		0.0908
KICH	64	1.369 (0.413 – 4.538)		0.6075
KIRC	539	0.456 (0.328 – 0.635)		3.2e-06
KIRP	289	0.593 (0.346 – 1.015)		0.0565
LGG	530	1.407 (1.068 – 1.853)		0.0150
LIHC	373	1.024 (0.765 – 1.369)		0.8749
LUAD	530	0.831 (0.638 – 1.082)		0.1696
LUSC	497	1.063 (0.768 – 1.471)		0.7115
MESO	84	0.795 (0.474 – 1.333)		0.3841
OV	379	1.174 (0.927 – 1.487)		0.1838
PAAD	179	0.656 (0.446 – 0.964)		0.0320
PCPG	184	0.937 (0.402 – 2.186)		0.8804
PRAD	501	0.946 (0.628 – 1.423)		0.7885
READ	166	1.069 (0.555 – 2.059)		0.8411
SARC	263	0.719 (0.517 – 1.001)		0.0506
SKCM	458	1.001 (0.801 – 1.251)		0.9935
STAD	372	0.876 (0.616 – 1.247)		0.4634
TGCT	139	0.980 (0.521 – 1.844)		0.9511
THCA	512	0.540 (0.309 – 0.944)		0.0306
THYM	119	0.818 (0.344 – 1.942)		0.6486
UCEC	553	0.934 (0.661 – 1.320)		0.6992
UCS	57	0.793 (0.411 – 1.529)		0.4889
UVM	79	1.220 (0.576 – 2.582)		0.6040

Figure 2 SETDB2-focused pan-cancer survival analyses. (**A**) Overall survival (OS). * p < 0.05, ** p < 0.01,*** p < 0.001. (**B**) Disease-specific survival (DSS). (**C**) Progression-free Interval curve.

SETDB2 Expression May Be a Prognostic and Diagnostic Biomarker for KIRC

The link between SETDB2 levels and KIRC patient outcomes was next examined based on TCGA data pertaining to KIRC patient survival. The resultant Kaplan-Meier curves indicated that patients expressing lower SETDB2 levels exhibited significantly worse OS (HR=0.58, p < 0.001) (Figure 5A), DSS (HR=0.43, p < 0.001) (Figure 5B), and PFI (HR=0.46, p < 0.001) relative to those expressing high levels of this gene (Figure 5C). These data emphasize the significant link between low levels of SETDB2 expression and poor KIRC patient prognostic outcomes.

ROC curves for SETDB2 yielded an AUC of 0.652, consistent with its efficacy when differentiating between KIRC tumors and healthy control tissues (Figure 5D). SETDB2 was also an effective biomarker suitable for identifying differently staged tumors, with respective AUC values of 0.615 for stage 1+2 and stage 3+4 KIRC (Figure 5E). In subgroup analyses, the utility of SETDB2 as a diagnostic biomarker was confirmed across multiple clinicopathological characteristics in KRIC patients, and a nomogram was established based on SETDB2 expression and other clinical parameters, thereby allowing for the prediction of KIRC patient 1-, 3-, and 5-year OS (Figure 5F). In conclusion, these results suggest that low SETDB2 levels are linked with poor prognosis in KIRC, providing an effective means of predicting outcomes in this cancer type.

SETDB2 Genetic Changes are Unrelated to KIRC Patient Survival

As mutations in particular genes are often linked with poor cancer patient outcomes,[20–22] SETDB2 gene mutations in KIRC patient samples were next analyzed with the cBioPortal database. Somatic mutations in SETDB2 were noted in 0.1% of KIRC samples, with just 2 such mutations in 30 samples, consisting primarily of missense mutations (Figure 6A). When cBioPortal was used for follow-up survival analyses of the relationships between SETDB2 and key KIRC hallmarks, these SETDB2 mutations were found to be unrelated to the prognosis of KIRC patients (Figure S1A and B). In the COSMIC database, SETDB2 mutation types were also assessed, revealing that missense mutations were present in ~2% of samples (Figure 6B). Of these mutations, 100% of substitutions were T > A (Figure 6C).
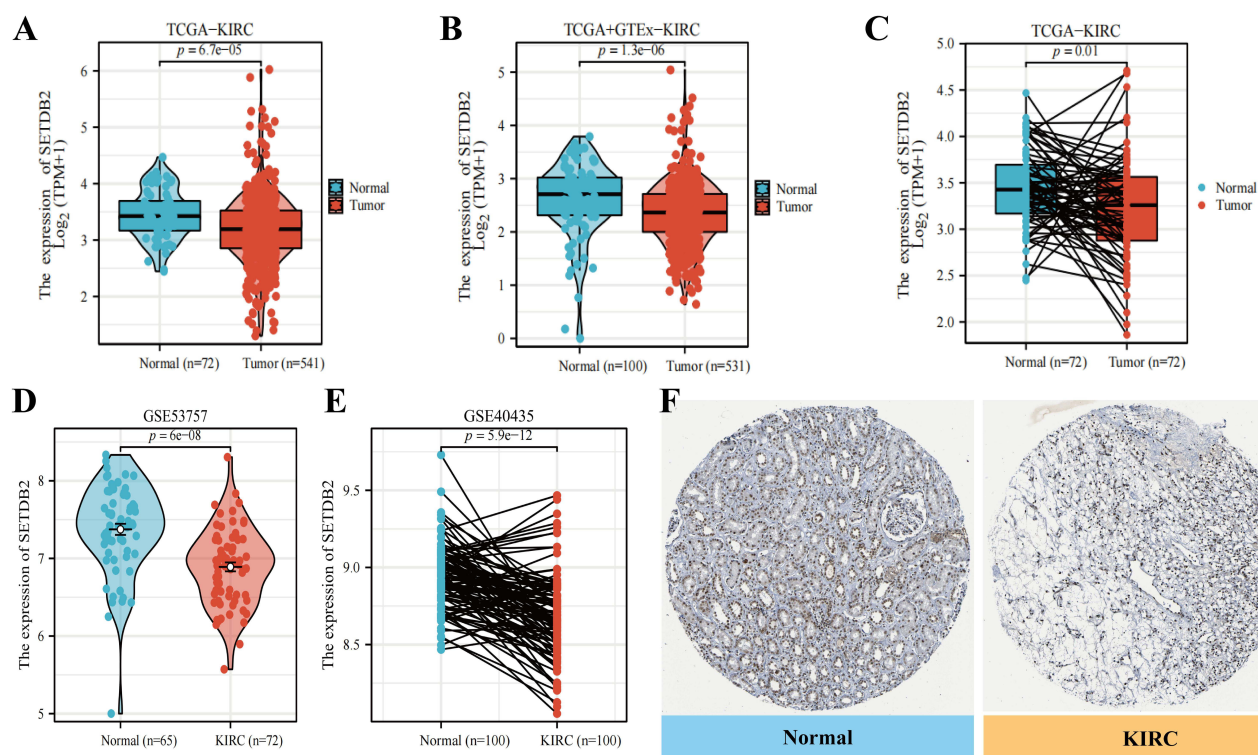
Figure 3 SETDB2 is downregulated in KIRC. (**A** and **B**) Comparison of SETDB2 between tumor and non-cancerous tissue samples in the TCGA-KIRC dataset (**A**) and the GTEX and TCGA databases (**B**). (**C**) Comparison of SETDB2 levels between tumors and paired paracancerous tissues in TCGA data. (**D**) Comparison of SETDB2 mRNA levels in KIRC tissues and control samples in the GSE53757 dataset. (**E**) SETDB2 mRNA expression in paired KIRC and controls from the GSE40435 dataset. (**F**) The HPA database was used to assess SETDB2 levels by immunohistochemical staining in paired KIRC and normal tissue samples.

Functional Enrichment of SETDB2-Related Genes in KIRC

To begin exploring the potential associations between SETDB2 and other proteins in KIRC tumors, a PPI network was established with STRING (Figure 7A). GEPIA2 was leveraged to aid in identifying the 200 genes most closely correlated with the expression of SETDB2. SETDB2 levels were observed to be positively associated with RCBTB1 expression (R = 0.830), GPALPP1 (R = 0.790), MEGF9 (R = 0.735), and SLC25A30 (R = 0.737) (Figure 7B). The two datasets were merged before GO and KEGG analyses. In KEGG analyses, SETDB2 was associated with "Lysine degradation" and the "Phosphatidylinositol signaling system" (Figure 7C), indicating that these may be related to its role in the oncogenic process. Key macromolecular processes identified through GO analyses included a range of biological processes such as macromolecule methylation, histone methylation, and general methylation. Enriched cellular components included chromatin silencing complexes, vesicle tethering complexes, and chromosomal regions, while enriched molecular functions included histone methyltransferase, protein methyltransferase, and histone-lysine N-methyltransferase activity.

Evaluation of SETDB2 Associations With KIRC Tumor Immune Infiltration

Links between SETDB2 and immune cell infiltration were next assessed with adjustment for tumor purity using the TIMER tool. SETDB2 levels in KIRC were found to be positively associated with tumor purity (R = 0.05, p = 2.88e−01), B cells (R = 0.271, p = 2.86e−06), CD8+ T cells (R = 0.187, p = 7.92e−05), CD4+ T cells (R = 0.338, p = 8.73e−14), macrophages (R = 0.487, p = 4.11e−28), neutrophils (R = 0.427, p = 1.13e−21), and DCs (R = 0.296, p = 1.25e−10) (Figure 8A). Corresponding analyses of the tumor microenvironment revealed that low levels of SETDB2 expression were associated with significantly lower stromal scores as compared to high levels of such expression (Figure 8B), although further experimental confirmation of these results is warranted. Differences in the immune cell proportions between the groups with low and high levels of SETDB2 expression were also compared. Significantly greater abundance of plasma cells, CD8+ T cells, follicular helper T cells, Tregs, and activated NK cells were observed in the
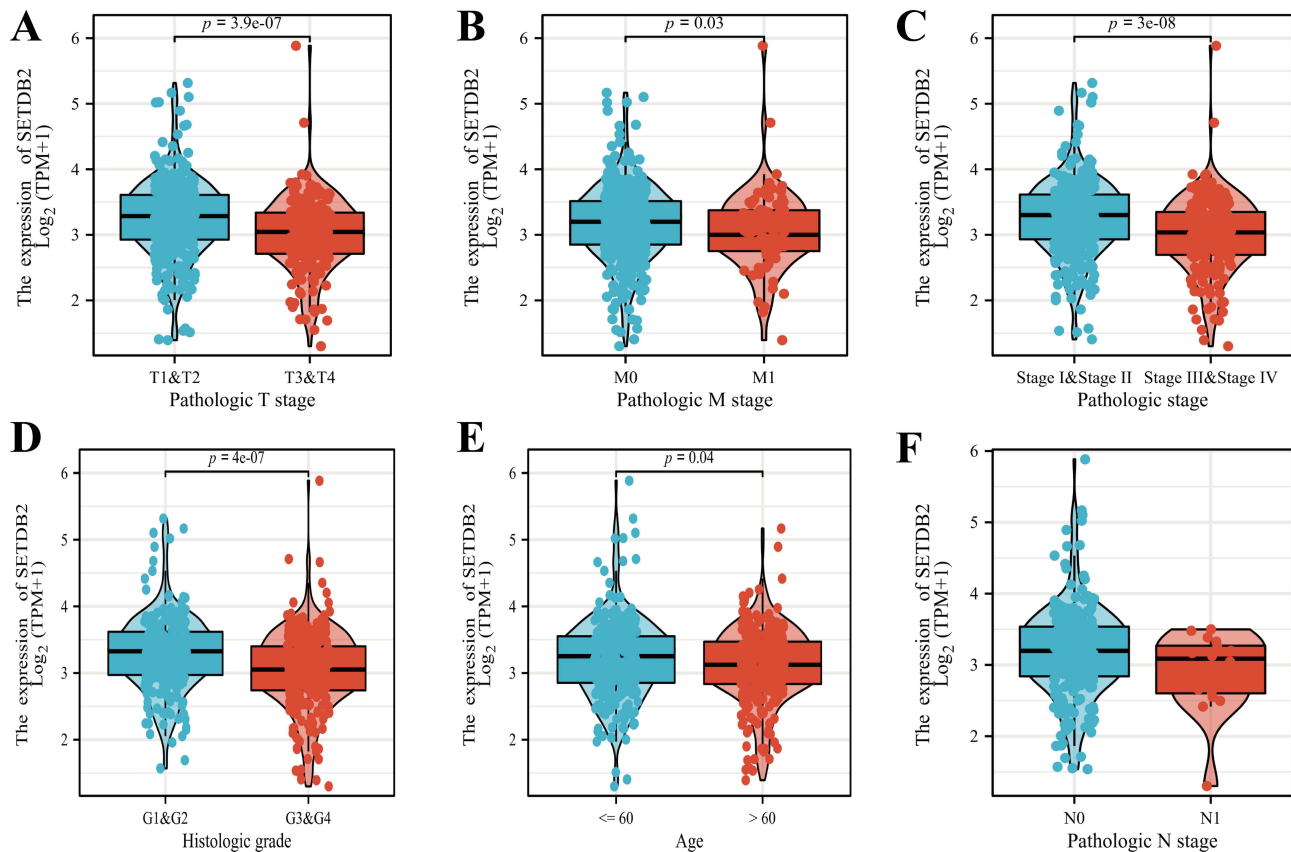
Figure 4 Relationships between SETDB2 levels and KIRC patient characteristics. (**A** and **B**, **F**) Pathologic T (**A**), M (**B**), and N (**F**) stages; (**C**) Pathologic stage; (**D**) Histologic grade; (**E**) Age.

group with low levels of SETDB2 expression relative to those with high levels of such expression (Figure 8C). Lastly, the association between SETDB2 levels and a range of immune cell types was performed (Figures 8D-F), revealing SETDB2 levels to be positively associated with monocytes (R = 0.257, p < 0.001) but negatively associated with regulatory T cells (Tregs) (R = −0.349, p < 0.001).

SETDB2 Negatively Regulates Cuproptotic Activity in KIRC Tumors

Cuproptosis is a form of cell death with close associations with cellular metabolic activity.[23–25] Glycolysis-dependent cells are better able to resist cuproptosis as compared to cells that depend on oxidative phosphorylation, suggesting that efforts to target glycolysis may help initiate cuproptosis.[26] Accordingly, the link between SETDB2 expression and cellular sensitivity to cuproptosis was next examined, leveraging the TCGA-KIRC dataset to detect correlations between the levels of this methyltransferase and genes known to be associated with cuproptosis, such as CDKN2A, DLD, DLAT, MTF1, LIAS, LIPT1, GLS, SLC31A1, ATP7A, FDX1, DLST, DBT, PDHA1, PDHB, ATP7B, and GCSH (Figure 9A).[27–29] These analyses noted significant association between SETDB2 levels and those of several genes related to cuproptosis, with a particularly strong positive correlation between the levels of SETDB2 and DBT (R = 0.694, p < 0.001) (Figure 9B).

When samples from the TCGA-KIRC dataset were stratified into groups expressing low and high levels of SETDB2, differentially expressed genes related to cuproptosis were detectable (Figure 9C). These genes included LIPT1, PDHB, LIAS, ATP7A, DLAT, PDHA1, MTF1, GLS, ATP7B, DLD, SLC31A1, FDX1, DLST, and DBT, all of which were significantly upregulated in the group expressing high levels of SETDB2 (p<0.05). SETDB2 may thus influence the progression of KIRC and prognostic outcomes for affected patients through its effects on cuproptotic regulation.
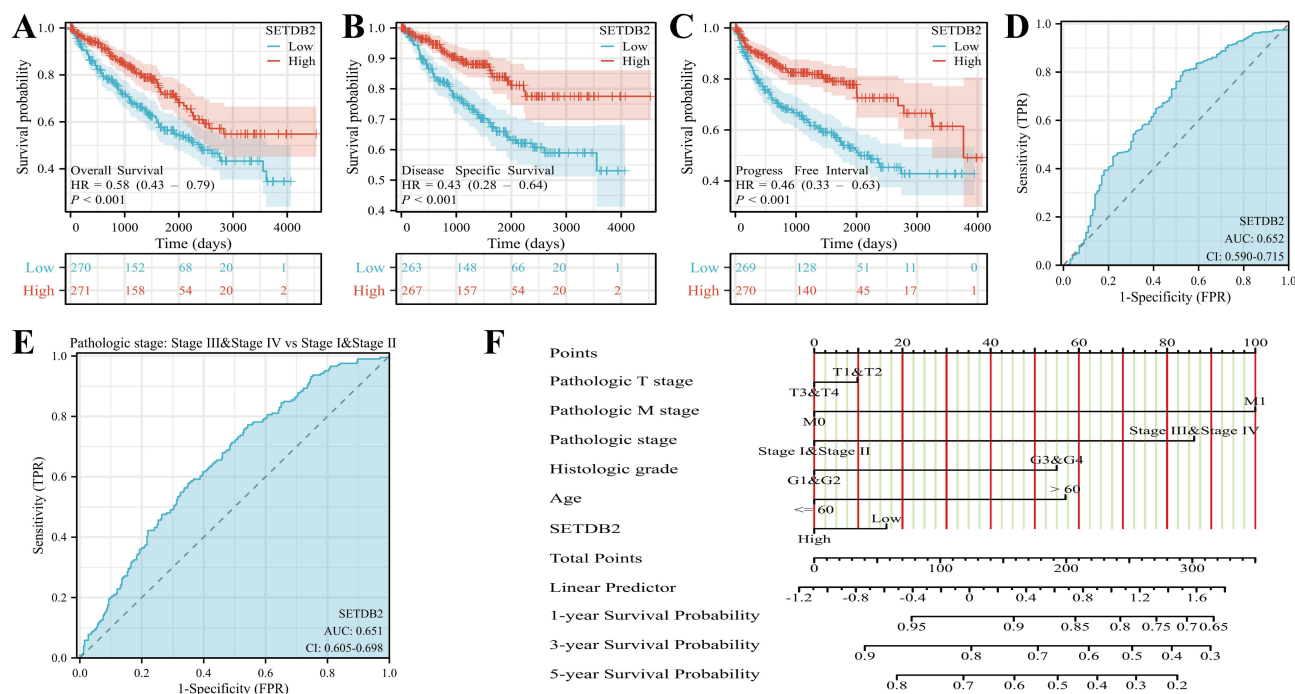
Figure 5 Evaluation of the prognostic and diagnostic performance of SETDB2 in KIRC patients. (**A-C**) Kaplan-Meier plots were used to compare the OS (**A**), DSS (**B**), and PFI (**C**) of KIRC patients as a function of their levels of SETDB2 expression (p < 0.05), with red and blue respectively corresponding to high and low SETDB2 levels. (**D**) ROC curves examining the ability of SETDB2 levels to differentiate between KIRC tumors and normal tissue. (**E**) ROC curves examining the ability of SETDB2 levels in distinguishing between KIRC tumors at different stages. (**F**) A developed nomogram to assess KIRC patient 1-, 3-, and 5-year OS based on SETDB2 expression and other clinicopathological parameters.

Molecular Docking Analysis for SETDB2

The comprehensive online analysis from the Genomics of Drug Sensitivity in Cancer revealed a significant positive correlation between the protein SETDB2 and the compound Lapatinib, with a correlation coefficient (cor) of 0.22 and a false discovery rate (FDR) of 1.08e-4 (Figure 10A). This correlation led to further investigation of the molecular interactions between these two entities, specifically focusing on the binding stability of Lapatinib and SETDB2. Molecular docking techniques were employed to explore these interactions; these are sophisticated computational methods that predict the preferred orientation of one molecule to another when forming a stable complex. Figure 10 presents the molecular docking analysis of SETDB2. Binding stability was evaluated based on binding energy, with values less than −5 kcal/mol indicating significant interactions, and values less than −7 kcal/mol indicating strong interactions.[30,31] The results of this molecular docking analysis indicated strong and significant binding interactions between Lapatinib and SETDB2 (Figure 10B and C). The calculated binding energy for this interaction was −7.90 kcal/mol, clearly surpassing the threshold for a strong binding interaction. This finding underscores the potential role of Lapatinib in modulating SETDB2 functions and highlights its potential as a therapeutic target in strategies against KIRC.

SETDB2 Upregulation Suppresses KIRC Cell Malignant Behaviors

To begin validating the above results, SETDB2 was successfully upregulated in two KIRC cell lines with an overexpression plasmid (Figure 11A and B). In CCK-8 assays, SETDB2 overexpression led to a significant decline in proliferative activity (Figure 11C). This coincided with significantly decreased metastatic potential for cells overexpressing SETDB2 in a wound healing assay (Figure 11D), and with significantly impaired invasivity in a Transwell assay (Figure 11E).

Discussion

Renal cell carcinoma cases account for more than 90% of all kidney cancers, and these are derived from the renal epithelium. KIRC is an extremely deadly kidney cancer subtype characterized by high levels of invasive growth,
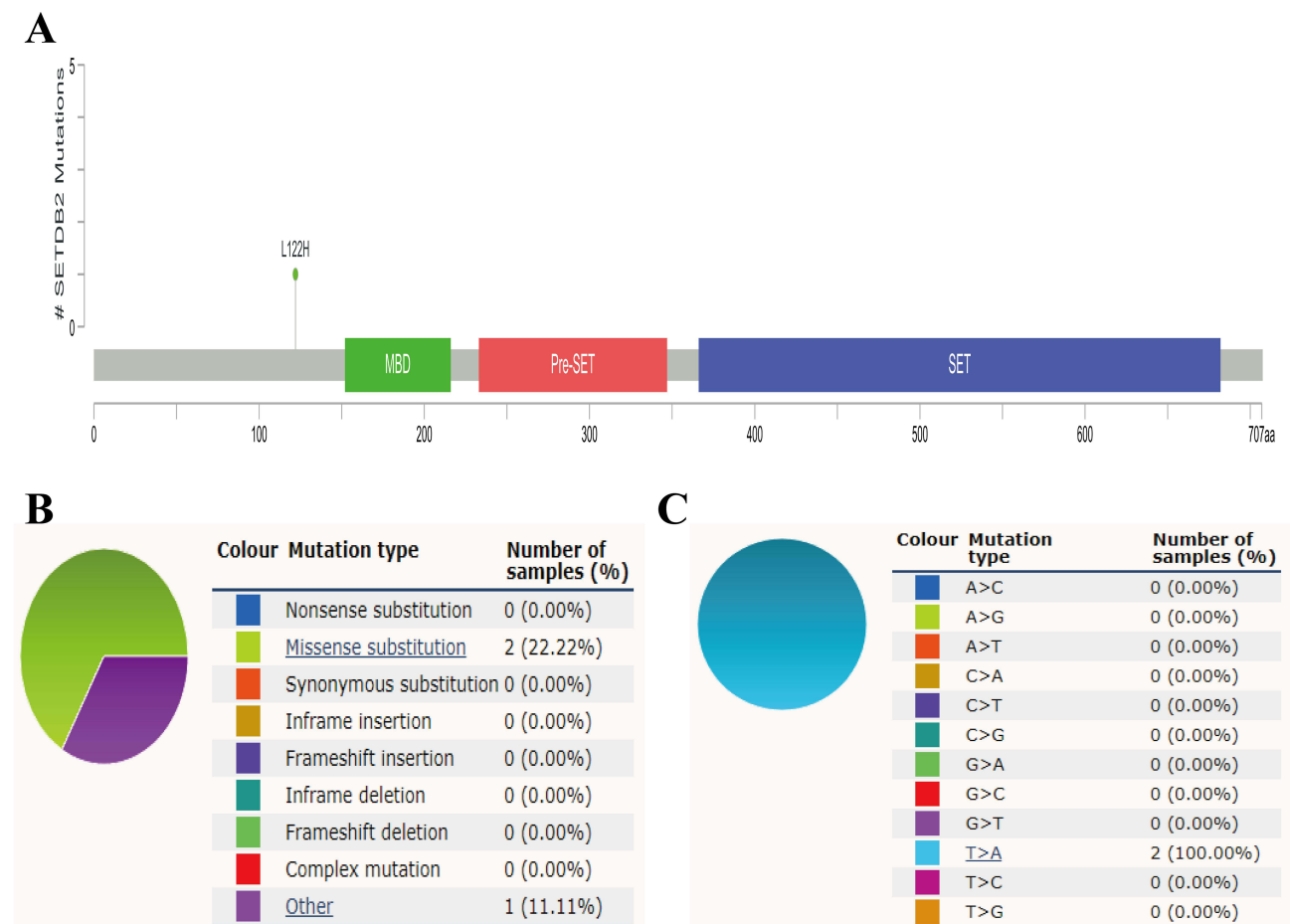
A

B

Colour	Mutation type	Number of samples (%)
	Nonsense substitution	0 (0.00%)
	Missense substitution	2 (22.22%)
	Synonymous substitution	0 (0.00%)
	Inframe insertion	0 (0.00%)
	Frameshift insertion	0 (0.00%)
	Inframe deletion	0 (0.00%)
	Frameshift deletion	0 (0.00%)
	Complex mutation	0 (0.00%)
	Other	1 (11.11%)

C

Colour	Mutation type	Number of samples (%)
	A>C	0 (0.00%)
	A>G	0 (0.00%)
	A>T	0 (0.00%)
	C>A	0 (0.00%)
	C>T	0 (0.00%)
	C>G	0 (0.00%)
	G>A	0 (0.00%)
	G>C	0 (0.00%)
	G>T	0 (0.00%)
	T>A	2 (100.00%)
	T>C	0 (0.00%)
	T>G	0 (0.00%)

Figure 6 Evaluation of the mutation status of SETDB2 in KIRC. (**A**) cBioPortal schematic showing the mutations of SETDB2 in KIRC. (**B** and **C**) COSMIC-based detection of SETDB2 mutation types.

metastasis, chemoresistance, and radioresistance.[32–35] Although significant progress has been made in the treatment of clear cell renal cell carcinoma in recent years, due to the heterogeneity of kidney cancer, there is considerable variation in how patients respond to treatment. Therefore, the establishment of alternative biomarkers for KIRC is crucial for aiding its diagnosis, improving patient prognostic outcomes, and designing more effective, targeted intervention strategies for affected patients. SETDB2 gene mutations have previously been linked to various diseases,[9,36,37] and the expression of SETDB2 can reportedly shape the development and progression of gastric cancer.[38–40] Studies of the expression, regulatory processes, and prognostic relevance of SETDB2 in KIRC, however, remain quite limited. In this study, the prognostic and functional relevance of SETDB2 were therefore explored in this cancer type through a series of thorough bioinformatics analyses supported by in vitro experimental results.

Here, low levels of SETDB2 expression were observed in KIRC, indicating that this methyltransferase may influence the onset and progression of this cancer type. The M1 and N1 stages of disease were associated with a significant reduction in SETDB2 levels relative to the corresponding M0 and N0 stages ($p < 0.05$), suggesting low SETDB2 expression to be strongly correlated with KIRC development, invasion, and metastatic progression. These results were consistent with the in vitro experiments conducted with KIRC cell lines. Other studies have similarly established SETDB2 as a prognostic biomarker related to the survival of lung adenocarcinoma patients.[41] In survival analyses performed herein, lower SETDB2 levels were associated with worse patient OS, PFI, and DSS, with consistent findings in subgroup-based prognostic analyses. The nomogram developed based on these findings may offer value as a tool to predict KIRC patient outcomes, underscoring its promise as a biomarker for this form of cancer that may assist efforts aimed at early diagnosis and patient treatment.
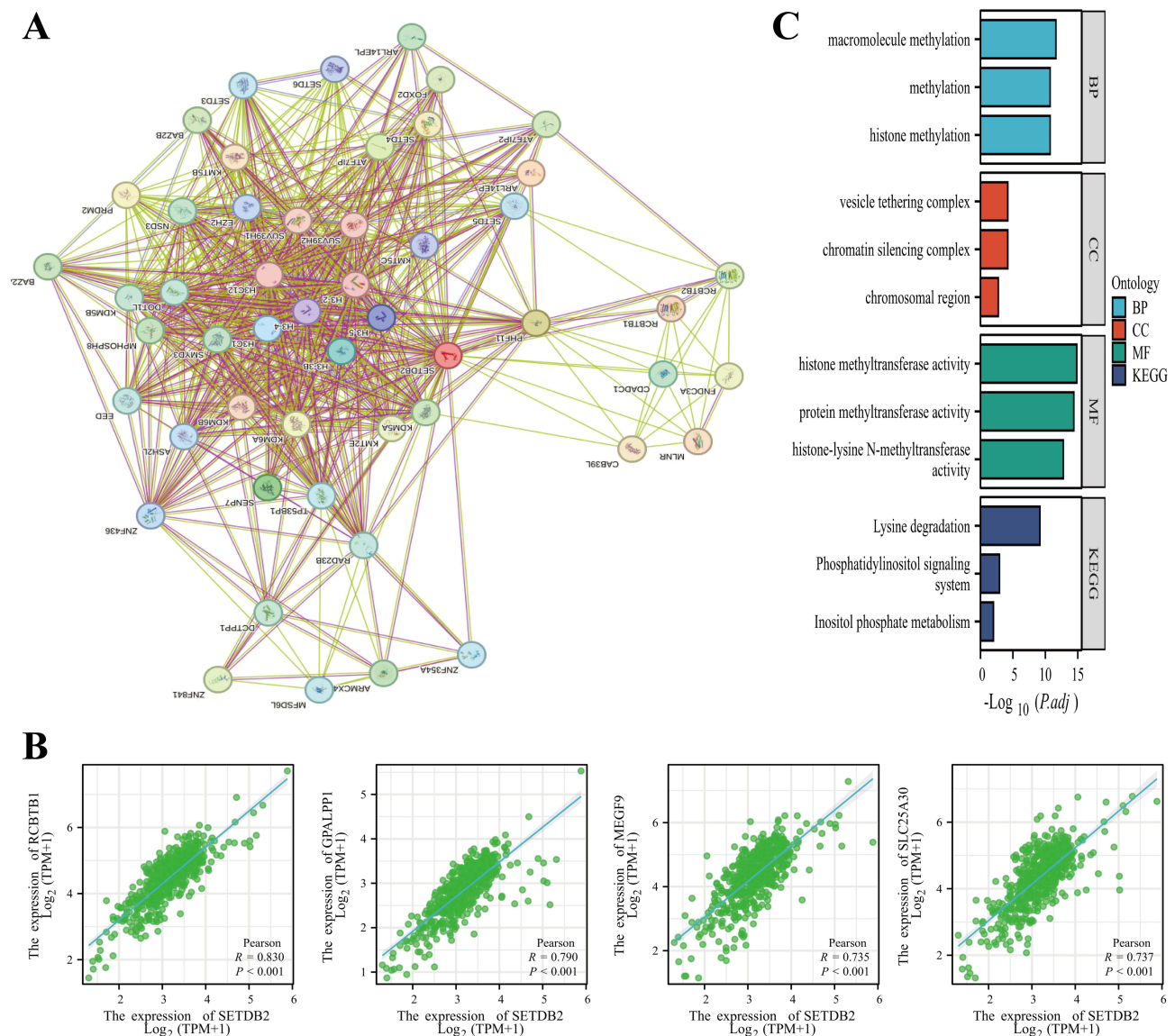
Figure 7 Functional enrichment analyses of genes associated with SETDB2 in KIRC. (**A**) A PPI network of putative proteins that interact with SETDB2 as established with the STRING tool. (**B**) Correlations between SETDB2 and the top four genes most closely correlated therewith in the TCGA dataset as analyzed via the GEPIA2 method. (**C**) GO and KEGG enrichment analyses of SETDB2-related genes.

GO and KEGG enrichment analyses of SETDB2-associated genes were also conducted to better understand the role it may play in KIRC. Through these analyses, a link was noted between SETDB2 and lysine degradation, the phosphatidylinositol signaling system, and a range of other biological processes. Phosphatidylinositol signaling activity is often dysregulated in the course of oncogenic progression, shaping the characteristics of tumor cells, including their motility and proliferation.[42–44] The downregulation of SETDB2 can also promote PI3K/Akt pathway-mediated alternative macrophage activation, attenuating NAFLD after sleeve gastrectomy.[45]

The key role that immunotherapy can play in KIRC has been demonstrated in several recent studies.[46,47] Accordingly, the association between SETDB2 and immune cell infiltration was further examined in this study, revealing SETDB2 levels to be significantly related to infiltration of immune cells including CD4+ T cells, CD8+ T cells, B cells, DCs, macrophages, and neutrophils into KIRC tumors. ESTIMATE data further supported a positive correlation between SETDB2 levels and stromal scores. SETDB2 thus appears to play a key role in the regulation of immune activity.

Higher immune checkpoint molecule expression levels tend to coincide with greater immune checkpoint inhibitor (ICI) efficacy.[48,49] In recent studies, ICIs have been shown to provide significant benefits to the survival of KIRC
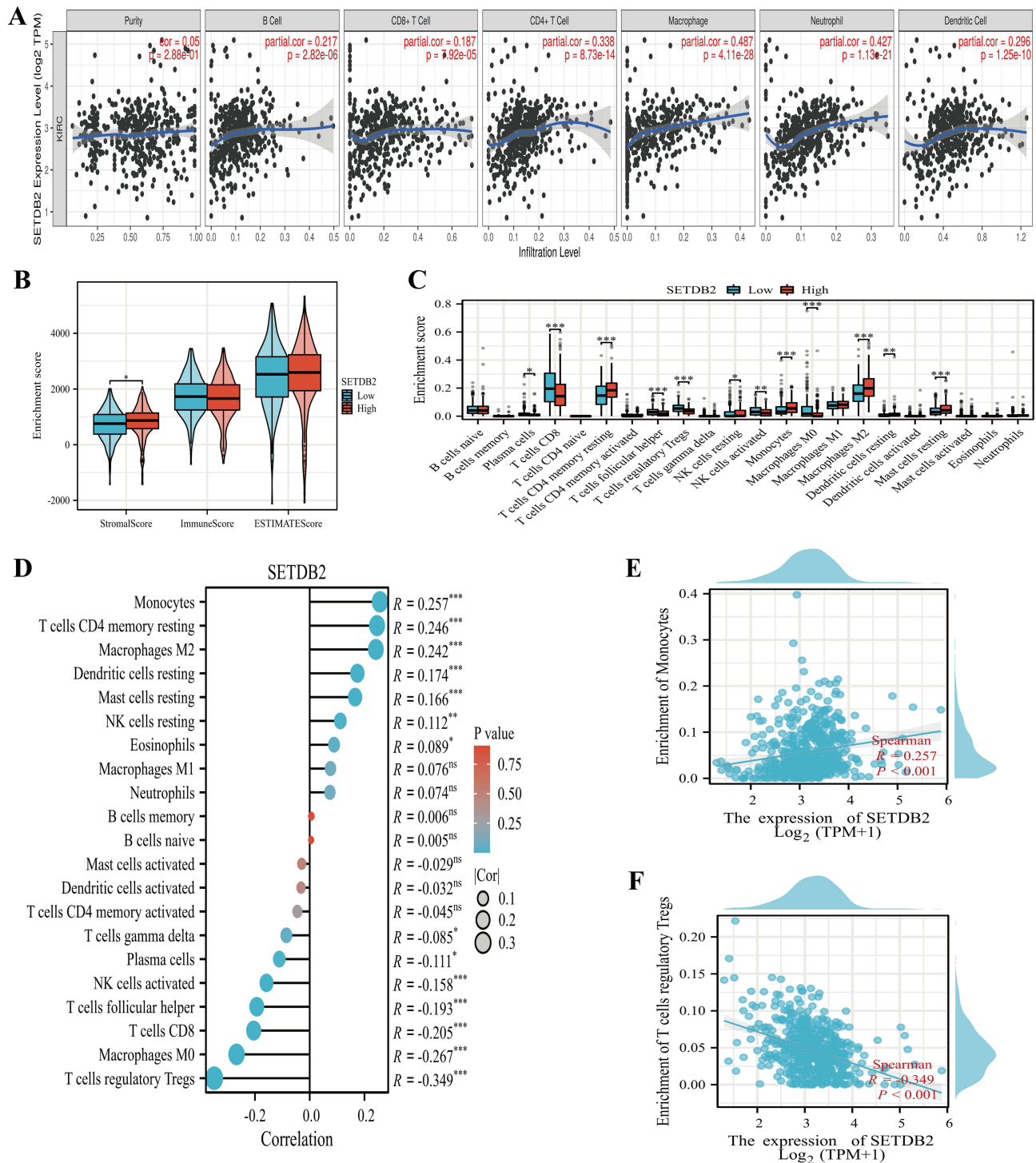
Figure 8 SETDB2 expression is associated with immune cell infiltration in KIRC tumors. (**A**) SETDB2 associations with tumor purity and immune cell infiltration. (**B**) Examination of SETDB2 correlations with KIRC immune, stromal, and ESTIMATE scores. (**C**) Associations between SETDB2 levels and immune cell infiltration. (**D**) Associations between SETDB2 levels and immune cell infiltration. (**E**) Correlations between SETDB2 levels and monocytes (**E**) and Tregs (**F**). ***p<0.001. NS, not significant.

patients,[50] with PD-L1 and CTLA4 being the most commonly studied and most clinically relevant checkpoint molecules in human cancers.[51] For this reason, the association between SETDB2 and immune checkpoints was also analyzed, revealing that it was positively correlated with the levels of both CD274 (PD-L1) as well as CTLA4 (Figure S2A), supporting the potential ability of SETDB2 to enhance ICI efficacy. TMB is also strongly correlated with tumor
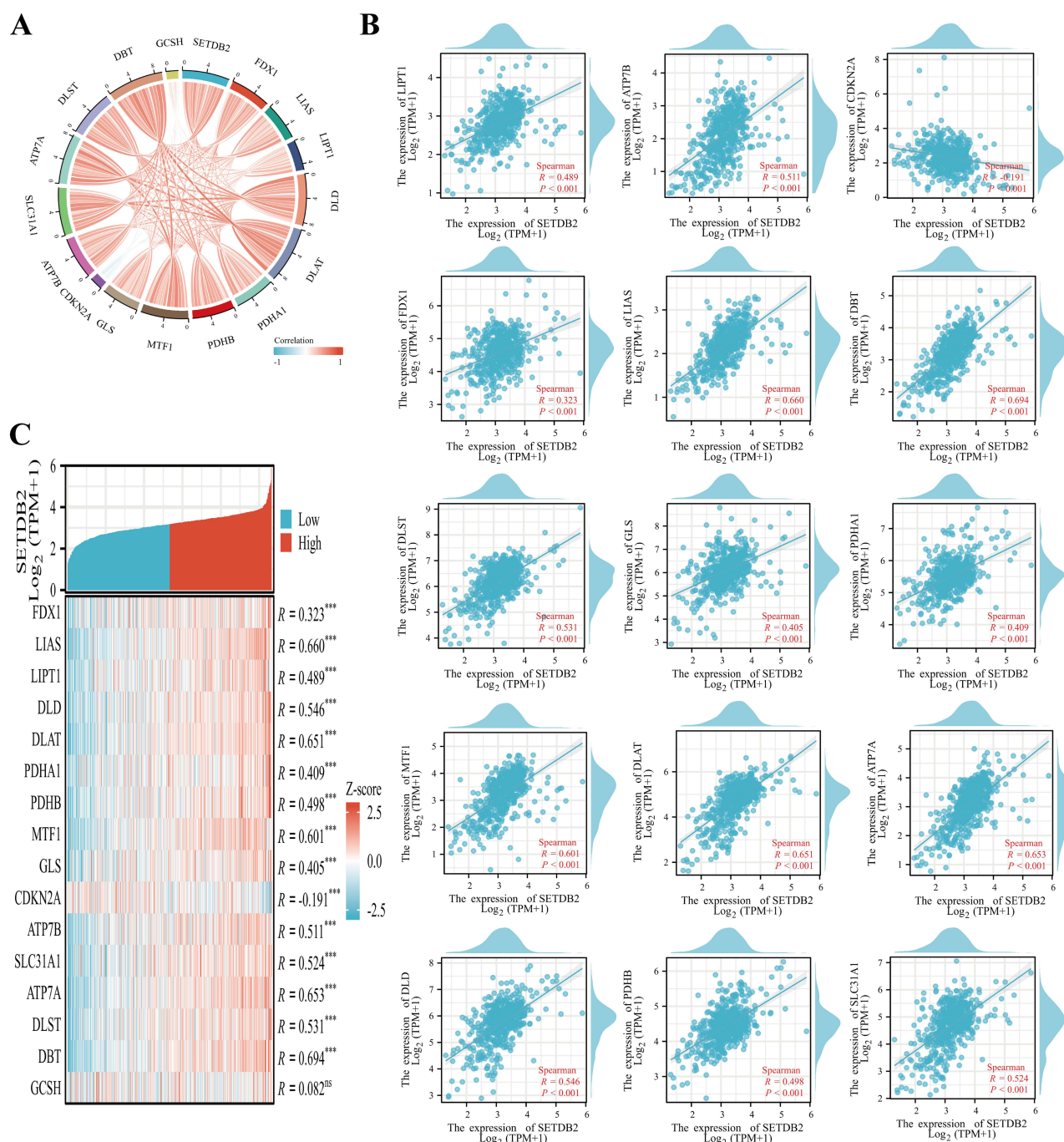
Figure 9 SETDB2 expression levels in KIRC tumors are related to levels of cuproptosis-related genes. (**A** and **B**) Correlations between SETDB2 expression and that of cuproptosis-related genes in the TCGA (**A**) and GEPIA2 (**B**) datasets. (**C**) Cuproptosis-related genes differentially expressed between the KIRC samples with low and high levels of SETDB2 expression. *p<0.05,**p<0.01,***p<0.001; NS, not significant.

neoantigen availability such that it is a key biomarker for the efficacy of ICI treatment.[52,53] SETDB2 has also been reported as a tumor-specific antigen in gastric cancer.[54] In KIRC, mutation analyses indicated that SETDB2 expression was significantly related to TMB according to data from the TCGA database (Figure S2B). Further studies of the promise of SETDB2 as a neoantigen in this form of cancer are thus warranted.

Copper nanoparticle-based treatments have been demonstrated to induce cuprotic activity in tumor cells, leading to enhanced DC maturation and antitumor CD8+ T cell infiltration.[55,56] Bioinformatics studies have increasingly
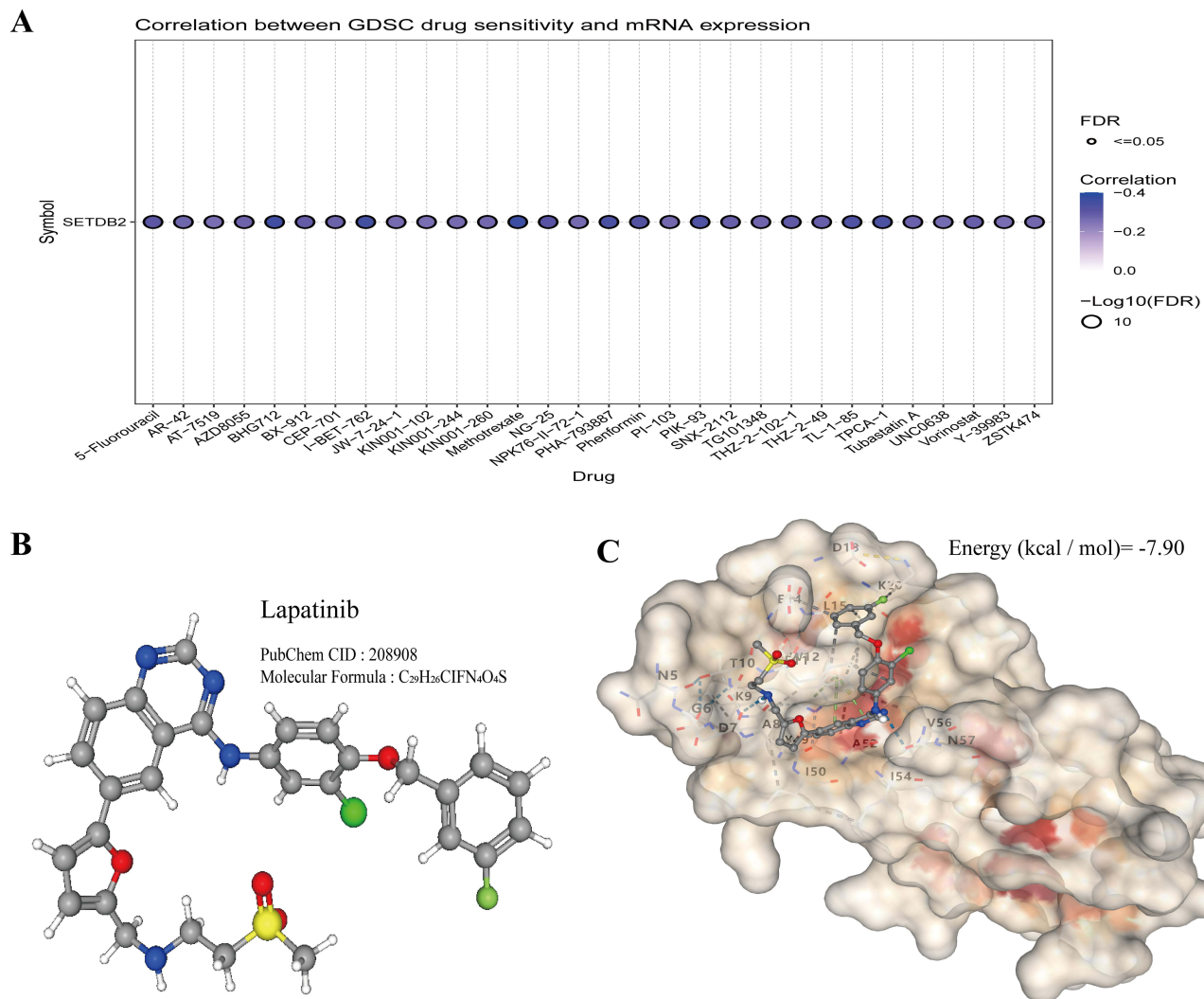
Figure 10 Molecular docking analysis for SETDB2. (**A**) Analysis of drug susceptibility of SETDB2 performed online by GSCA. (**B**) Molecular structure of Lapatinib. (**C**) Molecular docking between Lapatinib and SETDB2.

highlighted the important role that cuproptosis plays in the tumorigenic process, further contributing to the complex nature of immune evasion by tumors.[57,58] Cuproptosis and immunogenic phenotypes thus appear to be potentially linked to one another such that studies of cuproptosis have the potential to provide greater insight into the processes of tumor development and the remodeling of the tumor microenvironment. In light of the key role that SETDB2 plays in glycolysis and the establishment of immunosuppressive microenvironmental conditions, together with its contribution to metastatic progression,[59] the association between SETDB2 and cuproptosis was explored in greater detail. These analyses revealed SETDB2 levels to be positively correlated with cuproptosis-related genes, suggesting a link between SETDB2-mediated tumor suppression and the control of cuproptosis, potentially highlighting novel therapeutic avenues for the management of KIRC.

Lastly, two KIRC cell lines were herein used to upregulate SETDB2. Surch upregulation was found to hamper KIRC cell proliferation, survival, and invasivity. These findings support a role for SETDB2 as a regulator of the cell cycle in KIRC cells, suppressing tumor development, growth, invasion, and metastasis. SETDB2 may thus be an attractive target for the treatment of KIRC.

Despite the important insights afforded by the present study, there are nonetheless multiple limitations that remain to be addressed in the future. For one, this study was based on a series of bioinformatics and in vitro analyses, underscoring the requirement for the validation of its utility as an early-stage biomarker and/or general biomarker of KIRC in larger
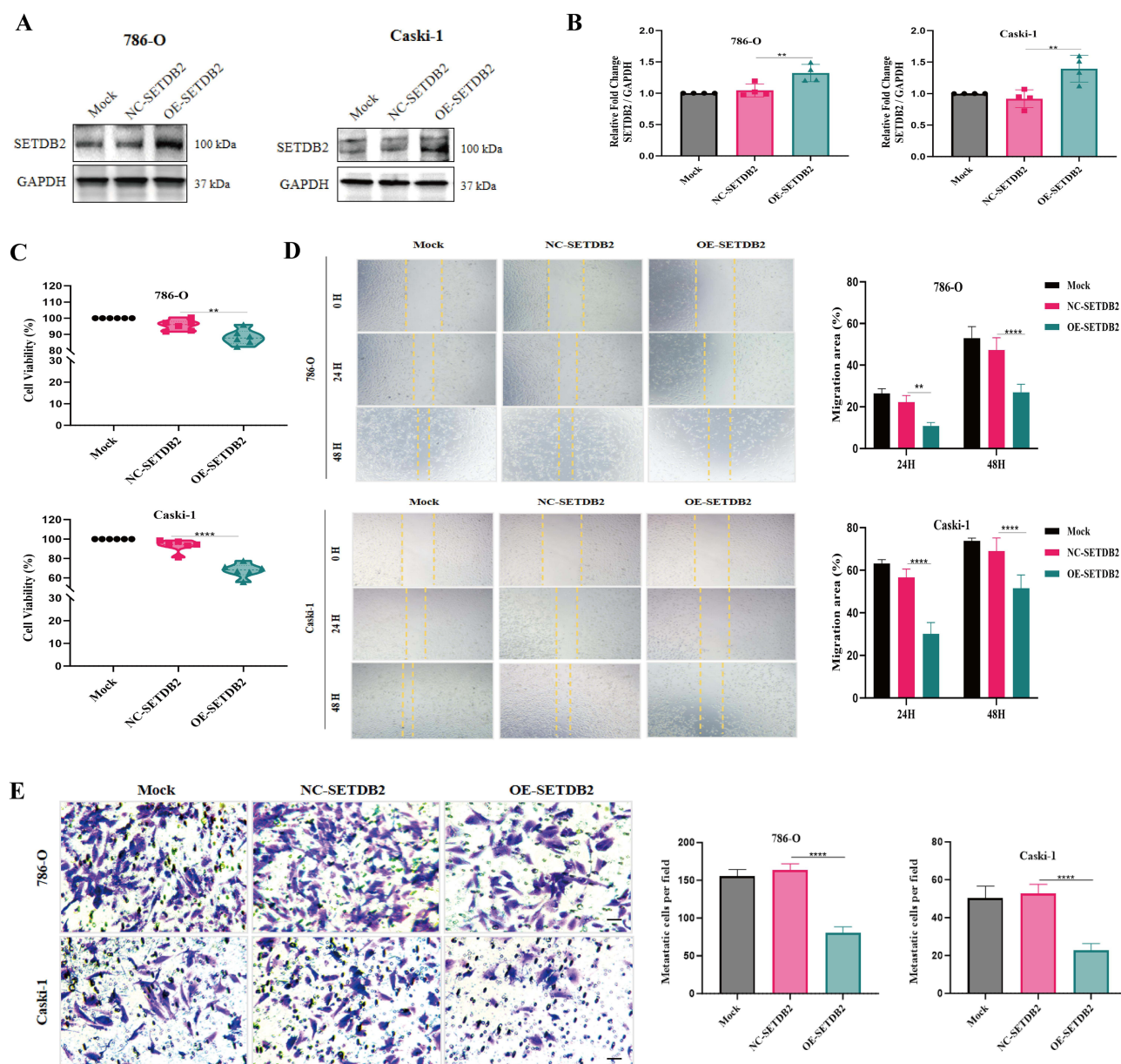
Figure 11 SETDB2 upregulation suppresses KIRC cell proliferative, migratory, and invasive activity. (**A** and **B**) Western blotting indicated increased SETDB2 expression in two KIRC cell lines following overexpression plasmid introduction (n=4). (**C-E**) SETDB2 upregulation was found to significantly suppress cellular proliferation (**C**), migration (**D**), and invasivity (**E**) in these cell lines (n=4-6). Scale bar = 50 μm. **p < 0.01, ****p < 0.001.

patient cohorts. Further validation of the precise mechanistic pathways through which SETDB2 is able to regulate immune cell infiltration and cuproptosis will also be required. Lastly, studies aimed at clarifying how targeting SETDB2 may influence anticancer treatment outcomes in vivo will be essential, and efforts to explore a range of drug combinations, including immunotherapies, are warranted.

In summary, SETDB2 downregulation may lead to the suppression and antitumor immunity, ultimately leading to KIRC onset, metastatic progression, and invasivity. SETDB2 expression levels are closely correlated with KIRC incidence such that they may be leveraged as a predictive biomarker for this disease. The interaction between Lapatinib and SETDB2 may elucidate KIRC-related mechanisms in clinical contexts. Overall, the present results will help advance the development of individualized and more efficacious treatment options for patients diagnosed with KIRC.

Data Sharing Statement

The data supporting this study are freely accessible through the TCGA data portal (https://portal.gdc.cancer.gov/projects/TCGA-KIRC) and the GSE53757 and GSE40435 datasets (http://www.ncbi.nlm.nih.gov/geo/). The authors had no special access privileges.

Ethics Statement

The Ethics Committee of Guizhou Nursing Vocational College reviewed the study and waived ethical approval requirements since the data were obtained from publicly available bioinformatics databases.

Acknowledgment

We are grateful to all co-authors of this study.

Author Contributions

All authors made a significant contribution to the work reported, whether that is in the conception, study design, execution, acquisition of data, analysis and interpretation, or in all these areas; took part in drafting, revising or critically reviewing the article; gave final approval of the version to be published; have agreed on the journal to which the article has been submitted; and agree to be accountable for all aspects of the work.

Funding

Disclosure

The authors report no conflicts of interest in this work.

References

1. Wang K, Ding Y, Liu Y. et al. Cpa4 as a biomarker promotes the proliferation, migration and metastasis of clear cell renal cell carcinoma cells. *J Cell mol Med*. 2024;28(7):e18165. doi:10.1111/jcmm.18165
2. Ljungberg B, Albiges L, Abu-Ghanem Y, et al. European association of urology guidelines on renal cell carcinoma: the 2022 update. *Eur Urol*. 2022;82(4):399–410. doi:10.1016/j.eururo.2022.03.006
3. Sung H, Ferlay J, Siegel RL, et al. Global cancer statistics 2020: globocan estimates of incidence and mortality worldwide for 36 cancers in 185 countries. *Ca Cancer J Clin*. 2021;71(3):209–249. doi:10.3322/caac.21660
4. Hsieh JJ, Purdue MP, Signoretti S, et al. Renal cell carcinoma. *Nat Rev Dis Primers*. 2017;3(1):17009. doi:10.1038/nrdp.2017.9
5. Bukavina L, Bensalah K, Bray F, et al. Epidemiology of renal cell carcinoma: 2022 update. *Eur Urol*. 2022;82(5):529–542. doi:10.1016/j.eururo.2022.08.019
6. Chen YW, Wang L, Panian J, et al. Treatment landscape of renal cell carcinoma. *Curr Treat Options Oncol*. 2023;24(12):1889–1916. doi:10.1007/s11864-023-01161-5
7. Henske EP, Cheng L, Hakimi AA, Choueiri TK, Braun DA. Chromophobe renal cell carcinoma. *Cancer Cell*. 2023;41(8):1383–1388. doi:10.1016/j.ccell.2023.07.006
8. Delahunt B, Eble JN, Egevad L, Samaratunga H. Grading of renal cell carcinoma. *Histopathology*. 2019;74(1):4–17. English. doi:10.1111/his.13735
9. Manuel R, Ryan ME, Peter EP, et al. Setdb2 links glucocorticoid to lipid metabolism t hrough insig2a regulation. *Cell Metab*. 2016;24(3): 474–84
10. Crespi B, Read S, Hurd P. The setdb2 locus: evidence for a genetic link between handedness and atopic disease. *Heredity (Edinb)*. 2018;120(1):77–82. doi:10.1038/s41437-017-0004-7
11. Nishikawaji T, Akiyama Y, Shimada S, et al. Oncogenic roles of the setdb2 histone methyltransferase in gastric cancer. *Oncotarget*. 2016;7(41):67251–67265. doi:10.18632/oncotarget.11625
12. Chen H, Ao Q, Wang Y, Qian Y, Cheng Q, Zhang W. Sox11 as a potential prognostic biomarker in hepatocellular carcinoma linked to immune infiltration and ferroptosis. *Chin J Cancer Res*. 2024;36(4):378–397. doi:10.21147/j.issn.1000-9604.2024.04.03
13. Zhao WJ, Ou GY, Lin WW. Integrative analysis of neuregulin family members-related tumor microenvironment for predicting the prognosis in gliomas. *Front Immunol*. 2021;12:682415. doi:10.3389/fimmu.2021.682415
14. Zhang W, Qiao XY, Li Q, et al. Comprehensive pan-cancer analysis of trpm8 in tumor metabolism and immune escape. *Front Oncol*. 2022;12:914060. doi:10.3389/fonc.2022.914060
15. Zhang W, Qian Y, Jin X, Wang Y, Mu L, Jiang Z. Sirt7 is a prognostic biomarker in kidney renal clear cell carcinoma that is correlated with immune cell infiltration. *Int J Gen Med*. 2022;15:3167–3182. doi:10.2147/IJGM.S353610

16. Liu K, Ma J, Ao J, et al. The oncogenic role and immune infiltration for carm1 identified by pancancer analysis. *J Oncol*. 2021;2021:2986444. doi:10.1155/2021/2986444

17. Meng ZY, Fan YC, Zhang CS, et al. Exosc10 is a novel hepatocellular carcinoma prognostic biomarker: a comprehensive bioinformatics analysis and experiment verification. *Peerj*. 2023:11:e15860. doi:10.7717/peerj.15860.

18. Liu CJ, Hu FF, Xia MX, Han L, Zhang Q, Guo AY. Gscalite: a web server for gene set cancer analysis. *Bioinformatics*. 2018;34(21):3771–3772. doi:10.1093/bioinformatics/bty411

19. Vijayakumar S, Manogar P, Prabhu S, Sanjeevkumar SR. Novel ligand-based docking; Molecular dynamic simulations; And absorption, distribution, metabolism, and excretion approach to analyzing potential acetylcholinesterase inhibitors for Alzheimer's disease. *J Pharm Anal*. 2018;8 (6):413–420. doi:10.1016/j.jpha.2017.07.006

20. Li J, Ran H, Zeng X, Yang D, Zeng X, Zhang P. Identification of hoxb9 based on comprehensive bioinformatics analysis for predicting prognosis of head and neck squamous cell carcinoma. *Medicine (Baltimore)*. 2023;102(35):e35035. doi:10.1097/MD.0000000000035035

21. Zhang M, Zhang J. Peg3 mutation is associated with elevated tumor mutation burden and poor prognosis in breast cancer. *Biosci Rep*. 2020;40(8). doi:10.1042/BSR20201648

22. Song J, Moscinski L, Zhang H, Zhang X, Hussaini M. Does sf3b1/tet2 double mutation portend better or worse prognosis than isolated sf3b1 or tet2 mutation? *Cancer Genomics Proteomics*. 2019;16(1):91–98. doi:10.21873/cgp.20115

23. Chen L, Min J, Wang F. Copper homeostasis and cuproptosis in health and disease. *Signal Transduct Target Ther*. 2022;7(1):378. doi:10.1038/s41392-022-01229-y

24. Xie J, Yang Y, Gao Y, He J. Cuproptosis: mechanisms and links with cancers. *mol Cancer*. 2023;22(1):46. doi:10.1186/s12943-023-01732-y

25. Sun L, Zhang Y, Yang B, et al. Lactylation of mettl16 promotes cuproptosis via m(6)a-modification on fdx1 mRNA in gastric cancer. *Nat Commun*. 2023;14(1):6523. doi:10.1038/s41467-023-42025-8

26. Wang D, Tian Z, Zhang P, et al. The molecular mechanisms of cuproptosis and its relevance to cardiovascular disease. *Biomed Pharmacother*. 2023;163:114830. doi:10.1016/j.biopha.2023.114830

27. Liu H. Pan-cancer profiles of the cuproptosis gene set. *Am J Cancer Res*. 2022;12(8):4074–4081.

28. Li J, Wu F, Li C, et al. The cuproptosis-related signature predicts prognosis and indicates immune microenvironment in breast cancer. *Front Genet*. 2022;13:977322. doi:10.3389/fgene.2022.977322

29. Feng S, Zhang Y, Zhu H, et al. Cuproptosis facilitates immune activation but promotes immune escape, and a machine learning-based cuproptosis-related signature is identified for predicting prognosis and immunotherapy response of gliomas. *Cns Neurosci Ther*. 2024;30(2): e14380. doi:10.1111/cns.14380

30. Chen P, Xie L, Ma L, Zhao X, Chen Y, Ge Z. Prediction and analysis of genetic effect in idiopathic pulmonary fibrosis and gastroesophageal reflux disease. *Iet Syst Biol*. 2023;17(6):352–365. doi:10.1049/syb2.12081

31. Li X, Zhou H, Ma R, et al. Structure of pou2af1 recombinant protein and it affects the progression and treatment of liver cancer based on wgcna and molecular docking analysis. *Int J Biol Macromol*. 2024;278(Pt 1):134629. doi:10.1016/j.ijbiomac.2024.134629

32. Argani P, Medeiros LJ, Matoso A, et al. "Oncocytoid renal cell carcinomas after neuroblastoma" represent tsc -mutated eosinophilic solid and cystic renal cell carcinomas: association with prior childhood malignancy and multifocality with therapeutic implications. *Am J Surg Pathol*. 2023;47(12):1335–1348. doi:10.1097/PAS.0000000000002101

33. Hu X, Tan C, Zhu G. Clinical characteristics of molecularly defined renal cell carcinomas. *Curr Issues mol Biol*. 2023;45(6):4763–4777. doi:10.3390/cimb45060303

34. Williamson SR. Renal cell carcinomas with a mesenchymal stromal component: what do we know so far? *Pathology*. 2019;51(5):453–462. doi:10.1016/j.pathol.2019.04.006

35. Albiges L, Flippot R, Rioux-Leclercq N, Choueiri TK. Non-clear cell renal cell carcinomas: from shadow to light. *J Clin Oncol*. 2018; JCO2018792531. doi:10.1200/JCO.2018.79.2531

36. Davis FM, Melvin WJ, Mangum K, et al. The histone methyltransferase setdb2 modulates tissue inhibitors of metalloproteinase-matrix metalloproteinase activity during abdominal aortic aneurysm development. *Ann Surg*. 2023;278(3):426–440. doi:10.1097/SLA.0000000000005963

37. Torrano J, Al EA, Hammerlindl H, Schaider H. Emerging roles of h3k9me3, setdb1 and setdb2 in therapy-induced cellular reprogramming. *Clin Clin Epigenet*. 2019;11(1):43. doi:10.1186/s13148-019-0644-y

38. Bayarkhangai B, Noureldin S, Yu L, et al. A comprehensive and perspective view of oncoprotein set in cancer. *Cancer Med*. 2018;7(7):3084–3094. doi:10.1002/cam4.1526

39. Hung MH, Chen KF. Reprogramming the oncogenic response: set protein as a potential therapeutic target in cancer. *Expert Opin Ther Targets*. 2017;21(7):685–694. doi:10.1080/14728222.2017.1336226

40. Liang X, Bao X, Chen G. Set protein in cancer: a potential therapeutic target. *Mini Rev Med Chem*. 2021;21(16):2290–2299. doi:10.2174/1389557521666210114163318

41. Yuan G, Hu B, Ma J, et al. Histone lysine methyltransferase setdb2 suppresses nrf2 to restrict tumor progression and modulates chemotherapy sensitivity in lung adenocarcinoma. *Cancer Med*. 2023;12(6):7258–7272. doi:10.1002/cam4.5451

42. Wang X, Deng Y, Gao L, et al. Series-temporal transcriptome profiling of cotton reveals the response mechanism of phosphatidylinositol signaling system in the early stage of drought stress. *Genomics*. 2022;114(5):110465. doi:10.1016/j.ygeno.2022.110465

43. Davis SE, Hopke A, Minkin SJ, Montedonico AE, Wheeler RT, Reynolds TB. Masking of beta(1-3)-glucan in the cell wall of candida albicans from detection by innate immune cells depends on phosphatidylserine. *Infect Immun*. 2014;82(10):4405–4413. doi:10.1128/IAI.01612-14

44. O'Donnell VB, Rossjohn J, Wakelam MJ. Phospholipid signaling in innate immune cells. *J Clin Invest*. 2018;128(7):2670–2679. doi:10.1172/JCI97944

45. Yu T, Wang L, Cheng Y, et al. Downregulation of setdb2 promotes alternative activation of macrophages via the pi3k/akt pathway to attenuate NAFLD after sleeve gastrectomy. *Biochem Biophys Res Commun*. 2024;726:150264. doi:10.1016/j.bbrc.2024.150264

46. Fang G, Wang X. Prognosis-related genes participate in immunotherapy of renal clear cell carcinoma possibly by targeting dendritic cells. *Front Cell Dev Biol*. 2022;10:892616. doi:10.3389/fcell.2022.892616

47. Bi K, He MX, Bakouny Z, et al. Tumor and immune reprogramming during immunotherapy in advanced renal cell carcinoma. *Cancer Cell*. 2021;39(5):649–661. doi:10.1016/j.ccell.2021.02.015

48. Puzanov I, Diab A, Abdallah K, et al. Managing toxicities associated with immune checkpoint inhibitors: consensus recommendations from the society for immunotherapy of cancer (sitc) toxicity management working group. *J Immunother Cancer*. 2017;5(1):95. doi:10.1186/s40425-017-0300-z

49. Wang SJ, Dougan SK, Dougan M. Immune mechanisms of toxicity from checkpoint inhibitors. *Trends Cancer*. 2023;9(7):543–553. doi:10.1016/j.trecan.2023.04.002

50. Fan Z, Sun X, Li K, et al. Construction and validation of a novel immune checkpoint-related model in clear cell renal cell carcinoma. *Dis Markers*. 2022;2022:9010514. doi:10.1155/2022/9010514

51. Zhang H, Dai Z, Wu W, et al. Regulatory mechanisms of immune checkpoints pd-l1 and ctla-4 in cancer. *J Exp Clin Cancer Res*. 2021;40(1):184. doi:10.1186/s13046-021-01987-7

52. Chan TA, Yarchoan M, Jaffee E, et al. Development of tumor mutation burden as an immunotherapy biomarker: utility for the oncology clinic. *Ann Oncol*. 2019;30(1):44–56. doi:10.1093/annonc/mdy495

53. Jardim DL, Goodman A, de Melo GD, Kurzrock R. The challenges of tumor mutational burden as an immunotherapy biomarker. *Cancer Cell*. 2021;39(2):154–173. doi:10.1016/j.ccell.2020.10.001

54. Choi YJ, Oh HR, Choi MR, et al. Frameshift mutation of a histone methylation-related gene setd1b and its regional heterogeneity in gastric and colorectal cancers with high microsatellite instability. *Hum Pathol*. 2014;45(8):1674–1681. doi:10.1016/j.humpath.2014.04.013

55. Guo B, Yang F, Zhang L, et al. Cuproptosis induced by ros responsive nanoparticles with elesclomol and copper combined with αPD-L1 for enhanced cancer immunotherapy. *Adv Mater*. 2023;35(22):e2212267. doi:10.1002/adma.202212267

56. Zhang C, Huang T, Li L. Targeting cuproptosis for cancer therapy: mechanistic insights and clinical perspectives. *J Hematol Oncol*. 2024;17(1):68. doi:10.1186/s13045-024-01589-8

57. Tong X, Tang R, Xiao M, et al. Targeting cell death pathways for cancer therapy: recent developments in necroptosis, pyroptosis, ferroptosis, and cuproptosis research. *J Hematol Oncol*. 2022;15(1):174. doi:10.1186/s13045-022-01392-3

58. Wendlocha D, Kubina R, Krzykawski K, Mielczarek-Palacz A. Selected flavonols targeting cell death pathways in cancer therapy: the latest achievements in research on apoptosis, autophagy, necroptosis, pyroptosis, ferroptosis, and cuproptosis. *Nutrients*. 2024;16(8):1201. doi:10.3390/nu16081201

59. Dai X, Jiang W, Ma L, et al. A metabolism-related gene signature for predicting the prognosis and therapeutic responses in patients with hepatocellular carcinoma. *Ann Transl Med*. 2021;9(6):500. doi:10.21037/atm-21-927